Nanoscale

PAPER

View Article Online
View Journal | View Issue

Cite this: *Nanoscale*, 2023, **15**, 9543

Enhanced catalytic performance derived from coordination-driven structural switching between homometallic complexes and heterometallic polymeric materials†

Gracjan Kurpik, [a,b] Anna Walczak, [a,b] Grzegorz Markiewicz, [a,b] Jack Harrowfield [c] and Artur R. Stefankiewicz *[a,b]

A bifunctional ligand 4,4-dimethyl-1-(pyridin-4-yl)pentane-1,3-dione (H**L**) able to provide two distinct coordination sites, *i.e.* anionic β-diketonate (after deprotonation) and neutral pyridine, has been used in the synthesis of Ag(I), Pd(II) and Pt(II) complexes that then have been applied as metalloligands for the construction of new heterometallic polymeric materials. The ambidentate nature of $\mathbf{L}^-$ enables switching between different modes of coordination within mononuclear complexes or their conversion into polymeric species in a fully controllable way. The coordination-driven processes can be triggered by various stimuli, *i.e.* a metal salt addition or acid–base equilibria, and presents an efficient strategy for the generation of metallosupramolecular materials. As a consequence of self-assembly, new multimetallic coordination aggregates have been synthesized and characterized in depth in solution (^{1}H NMR, ESI-MS) as well as in the solid state (XPS, SEM-EDS, FTIR, pXRD, TGA). Furthermore, the Pd-based assemblies have been found to be efficient catalyst precursors in the Heck cross-coupling reaction, demonstrating a direct impact of compositional and morphological differences on their catalytic activity.

Received 21st March 2023,
Accepted 1st May 2023

DOI: 10.1039/d3nr01298k

rsc.li/nanoscale

Introduction

Metal–ligand interactions are the primary driving force in the generation of simple coordination compounds, as well of metallosupramolecular architectures with a high degree of complexity and a precisely defined structure.[1] Taking into account the character of a coordinate bond, *i.e.* its high strength but commonly dynamic nature, coordination-driven self-assembly processes are characterized by high controllability at the molecular level with respect to directionality, reversibility and post-synthetic switchability.[2] The supramolecular transformations induced by different external physicochemical stimuli, *e.g.* changes in concentration,[3,4] acid–base equilibria,[5,6] stoichiometry,[7,8] cation/anion exchange,[9,10] or radiation,[11,12] lead to entirely new systems of diverse chemical composition, structure, topology and properties. Thus, externally driven interconversion processes and other structural modifications play an increasingly important role in the design and construction of functional materials that constitute a competitive approach to classical synthesis.[2,13]

Ambidentate pyridyl-β-diketonate ligands derived from pyridyl-1,3-diketones are an interesting class of organic species commonly used as building blocks in coordination and metallosupramolecular chemistry.[14–16] Such units are capable of binding metal-ion centers in more than one way through different donor-atom combinations. The distinct nature of coordination sites, *i.e.* anionic β-diketonate and neutral pyridine, makes them good donors for a wide range of metal cations, both hard and soft acids according to HSAB theory.[17,18] In most cases, they act as *O*,*O*-chelates or as simple N-donors through the pyridine ring, but other coordination modes can be achieved.[19,20] Due to this structural variety they have found a number of applications in the construction of sophisticated coordination assemblies, including complex compounds,[21–24] macrocycles,[14] multimetallic polymers,[20,25,26] metal–organic frameworks (MOFs)[27,28] and metallocages.[29–31]

Although a number of reports on metallosupramolecular assemblies based on pyridyl-β-diketonate-derived ligands are available in the literature, we focused on an unexplored aspect, namely the switchable nature of species with such units as

[a]*Center for Advanced Technology, Adam Mickiewicz University in Poznań, Uniwersytetu Poznańskiego 10, 61-614 Poznań, Poland. E-mail: ars@amu.edu.pl*
[b]*Faculty of Chemistry, Adam Mickiewicz University in Poznań, Uniwersytetu Poznańskiego 8, 61-614 Poznań, Poland*
[c]*Institut de Science et d'Ingénierie Supramoléculaires, Université de Strasbourg, 8 allée Gaspard Monge, 67083 Strasbourg, France*

†Electronic supplementary information (ESI) available. CCDC 2244267. For ESI and crystallographic data in CIF or other electronic format see DOI: https://doi.org/10.1039/d3nr01298k

well as conducting studies on the application potential of new heterometallic aggregates. In this work the ditopic molecule 4,4-dimethyl-1-(pyridin-4-yl)pentane-1,3-dione (**HL**) was employed to synthesize a series of Ag(I), Pd(II) and Pt(II) coordination compounds which were further converted into more complex metallosupramolecular assemblies. Particular efforts have been undertaken to ensure an efficient strategy for multistage supramolecular transformations between the resultant systems triggered by external stimuli. The present work describes coordination-driven structural switching between a variety of mononuclear complexes based on the ligand **HL**/**L**$^-$ and Ag(I), Pd(II) and Pt(II) cations. As a consequence of metallosupramolecular self-assembly, new heterometallic polymeric materials have been obtained and their physicochemical characterization is described ahead. Additionally, the diversity in their functionality has been illustrated by their use as catalyst precursors in the Heck cross-coupling reaction.

Results and discussion

Synthesis and characterization of complexes

As shown in Fig. 1, the pyridyl-β-diketone ligand **HL** acts as the starting material and main building block for all coordination species presented. Its ambidentate nature was used to design, obtain and convert a series of complexes with Ag(I), Pd(II) and Pt(II) cations. All the coordination compounds presented herein can be directly synthesized by complexation reactions between **HL** and appropriate metal salts. Pd(II) and Pt(II) complexes, *i.e.* $[Pd(HL)_4](NO_3)_2$ (**C3**), $[Pt(HL)_4](NO_3)_2$ (**C4**) and $[PdL_2]$ (**C6**) were synthesized according to literature procedures.[22,23] The compound $[Ag(HL)_2]NO_3$ (**C1**) was synthesized by the reaction of **HL** (2 equiv.) with $AgNO_3$ (1 equiv.) carried out in DCM/EtOH (1 : 1, v/v) at room temperature for 18 h. The generation and purity of the desired complex were confirmed in solution *via* ^{1}H NMR spectroscopy and ESI-MS spectrometry (Fig. S1 and S2†). Moreover, slow evaporation of the methanol solution provided crystals, suitable for single-crystal X-ray diffraction measurements. The complex **C1** crystallizes in the monoclinic space group $P2_1/n$ and has an almost ideal linear geometry of Ag(I) coordination where the N–Ag–N angle is equal to 170.53°. It is worth emphasizing that **C1** occurs as a dimer in the crystal (Fig. S13†), where two molecules are linked by a weak metal–metal interaction Ag···Ag (3.08 Å),[32,33] but this was not confirmed in solution. The β-diketone units remained in their protonated enol form and were not involved in the formation of coordinate bonds. The crystal and structure refinement data are given in the ESI, Table S1.†

Two structurally distinct Pd(II) complexes of the ligand **HL** and ethylenediamine (en) co-ligand were observed in solution *via* ^{1}H NMR spectroscopy but neither could be isolated in pure form. The reaction of $[Pd(en)(NO_3)_2]$ with 2 equiv. of **HL** in CD_3CN resulted in the formation of $[Pd(en)(HL)_2](NO_3)_2$ (**C2**) whereas the deprotonation of **HL** (1 equiv.) with Et_3N prior to the addition of metal salt gave $[Pd(en)L]NO_3$ (**C5**). Hence, depending on the reaction conditions applied one or two molecules of the ligand **HL** occupy two available positions in Pd(II) sphere and coordinate by *O*,*O*-chelate or N-donors, respectively. ^{1}H NMR spectroscopy as well as ESI-MS spectrometry allowed unequivocal determination of the structures and molecularity of the new compounds generated (Fig. S3–S6†).

Structural switching

In addition to their direct syntheses, the complexes can be converted into other species by addition of either appropriate metal salts or acid/base, as shown by ^{1}H NMR spectroscopy (Fig. 2 and see ESI, Fig. S14–S19†). As previously mentioned, the ligand **HL** reacted with $AgNO_3$ to give the disubstituted

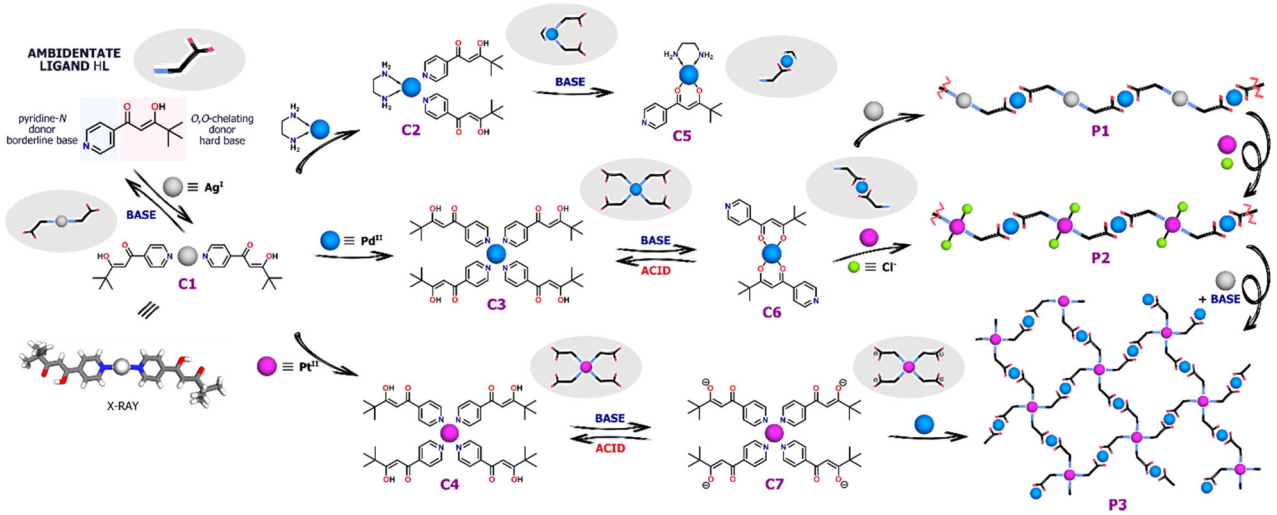

Fig. 1 General scheme showing the supramolecular transformations within coordination-driven assemblies based on Ag(I), Pd(II) and Pt(II) ions and the pyridyl-β-diketonate ligand HL.

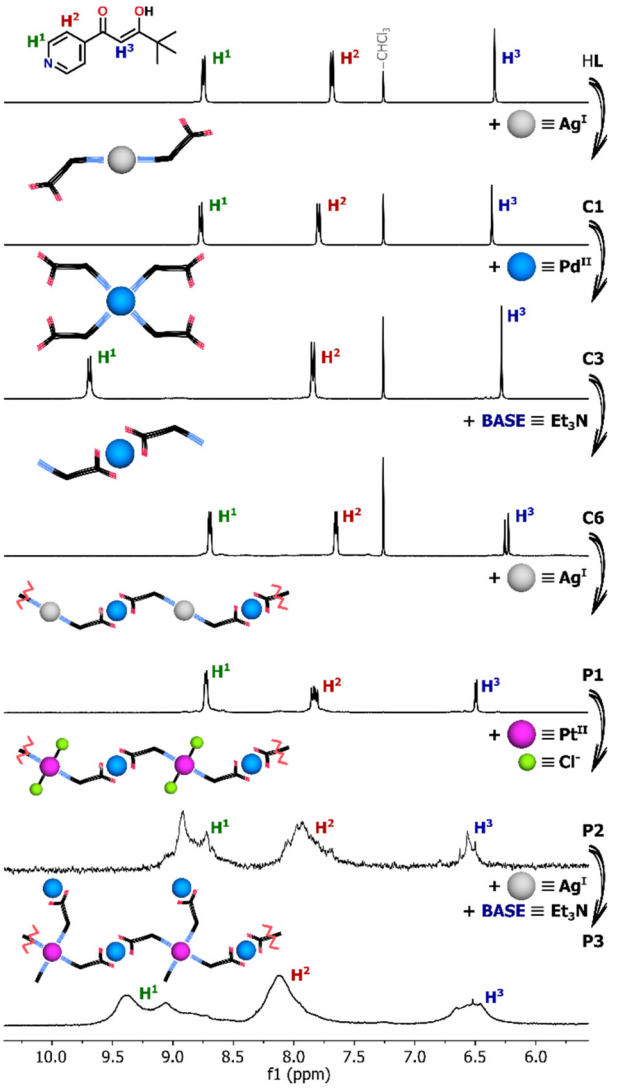

Fig. 2 Parts of ^{1}H NMR spectra (600 MHz, $CDCl_3$ or DMSO-d_6 for **P1–P3**) showing the coordination-driven transformations triggered by the addition of metal salt or base.

coordination compound **C1** although it decomposes under the influence of base (Fig. S14†). After addition of 0.5 equiv. of Et_3N only upfield shifted signals from the deprotonated ligand $\mathbf{L}^-$ were observed. Therefore, the instability of **C1** under basic conditions excluded its further coordination through *O,O*-chelation requiring prior deprotonation.

Nevertheless, the Ag(I) complex **C1** can be completely transformed into Pd(II) or Pt(II) species upon addition of the appropriate metal salt. As a result of $Pd(NO_3)_2$ addition, gradual disappearance of the **C1** signals was observed, along with the emergence of new intense signals for the Pd(II) compound, which was found to be the four-coordinate complex **C3** (Fig. S15†). As shown by ^{1}H NMR titration experiments, the change in the coordination number from 2 to 4 was clearly illustrated by the significantly downshifted signal ($\Delta\delta$ = ~0.8 ppm) from the protons near pyridine-N atoms (H^1). Similar behavior was observed when **C1** was titrated with [Pd(en)$(NO_3)_2$]. Two molecules of the ligand **HL** derived from the degradation of the Ag(I) complex completed the coordination sphere of Pd(II) leading to the formation of the heteroleptic compound **C2** (Fig. S16†).

In contrast, no additional signals or shifts were initially detected during the transformation of **C1** triggered by Pt(II) ions. The Ag(I) complex appeared to be stable as $Pt(NO_3)_2$ was added, not undergoing any obvious reaction. The generation of the desired complex **C4** was noticed only after several days due to the greater kinetic inertness of Pt(II) ion in comparison to Pd(II), for which no kinetic hysteresis was observed during the experiment (Fig. S17 and S18†).

The Pd(II) and Pt(II) coordination compounds generated by these metal ion exchange reactions of **C1** were subjected to the addition of base (Et_3N). Pd(II) complexes **C3** and **C6** can be easily interconverted between N- and O,O-donor forms with 100% efficiency by deprotonation/protonation of the enolic centre.[22] Addition of base to the cationic N-bound complex **C3** leads to linkage rearrangement and formation of neutral *O,O*-chelated counterparts, a reaction which can be reversed by addition of methanesulfonic acid (MSA). Similarly, titration of the heteroleptic species **C2** with Et_3N caused a change in the coordination mode *via* release of one N-bound ligand molecule and the formation of monocharged complex **C5** (Fig. S19†). No further transformation into the homoleptic complex **C6** coordinated by two β-diketonate units occurred despite the addition of a large excess of Et_3N (10 equiv.), consistent with the high stability of the Pd(en) unit. In contrast to its Pd(II) analogue, the Pt(II) complex **C4** does not undergo any conversion under basic conditions even after several days. The switching between cationic and neutral species is completely retarded by the kinetic inertness of Pt(II). Addition of a stoichiometric amount of Et_3N results only in deprotonation of the uncoordinated enol units and formation of anions $[Pt\mathbf{L}_4]^{2-}$ (**C7**), while the N-bound complex structure remains essentially intact.[23]

Synthesis of heterometallic polymers

Due to the presence of accessible coordination sites capable of reacting with metal cations, the complexes **C6** and **C7** (the deprotonated form of **C4**) can act as metalloligands. As a pyridine-N donor, Pd(II) complex **C6** was expected to be a good ligand for Ag(I) and for this reason **C6** was reacted with AgOTf (or $AgNO_3$) in anticipation of the formation of a new multimetallic aggregate $[PdAg_x\mathbf{L}_2]_n^{x+}$ (**P1**), where $x \approx 1$. In this structure, the *O,O*-chelating and pyridine-N donors were expected to be involved in coordination with Pd(II) and Ag(I), respectively, with Ag(I) being two-coordinate, as in complex **C1**. During a ^{1}H NMR titration of **C6** with AgOTf, a progressive decrease in signal intensity was observed as a result of the precipitation of a new product (Fig. S20–S21†) along with minor downfield chemical shifts that could be attributed to the coordination of Ag(I) cations by pyridine-N. Full disappearance of ^{1}H NMR signals from the Pd(II) metalloligand **C6** and complete product

precipitation (**P1**) were observed after the addition of 1 equiv. of Ag(I), corresponding to the expected reaction stoichiometry.

Next, **C6** was reacted with an equimolar amount of $PtCl_2$ in the expectation that retention of the chlorido ligands would favor formation of Pt(II) centers involving just two pyridine-N donors.[34,35] The reaction was performed in MeCN at 80 °C for 24 h, giving an orange precipitate, consistent with the formation of a coordination polymer **P2**. In order to verify the composition of the aggregate, we synthesized an analogue of the complex **C6** – $[Pd(bpm)_2]$,[36] which lacks pyridyl donors. In the control experiment, Pt(II) salt was added to the solution of $[Pd(bpm)_2]$ under the reaction conditions, but no clear changes were observed in the ^{1}H NMR spectra (Fig. S23†). Thus, the Pd/Pt exchange could be unambiguously excluded in the structure of the monomer **C6**, confirming the preservation of *O*,*O*-coordination for Pd(II) ions. The isolated material **P2** was highly insoluble in most common solvents and only in DMSO-d_6 it was possible to record ^{1}H NMR spectrum which showed severely broadened signals, indicative of the generation of the complex metalloaggregates in this solvent (Fig. S9†).

The capacity to deprotonate the enol units of **C4** without causing complex decomposition or isomerization prompted us to react **C7** with $Pd(NO_3)_2$ under basic conditions. The formation of a new species (**P3**) was observed and again broad and highly overlapped set of signals for all of the aromatic and methine protons were observed in the ^{1}H NMR spectrum (Fig. S11†). This broadening is characteristic of and consistent with the presence of complex metallosupramolecular assemblies. The spectrum contained no signal from the enol group of a diketone moiety (≈16 ppm), indicating complete coordination between this group and Pd(II), possibly as a result of the creation of a complex branched oligomeric structure. The control experiment carried out for a simple Pt(II) complex with pyridine ligands also excluded the exchange of inert Pt(II) ions with Pd(II). As indicated by the ^{1}H NMR spectra (Fig. S24†), its structure was retained in the reaction environment, which showed that only deprotonated *O*,*O*-chelates could be involved in the Pd(II) coordination.

The coordination-driven switching strategies developed for the mononuclear complexes **C1–C7** were successfully adapted to the transformations of the coordination polymers **P1–P3** as well. In order to exchange Ag(I) cations with Pt(II), $PtCl_2$ was added to the solution of **P1** in DMSO-d_6, which resulted in the precipitation of AgCl and a clear color change. The transformation, followed by ^{1}H NMR spectroscopy, indicated the formation of a new coordination complex, as illustrated by the significant broadening of downshifted signals in a spectrum consistent with that of **P2**. Furthermore, the polymer **P2** was converted into **P3** in a two-step process by adding $AgNO_3$ and, subsequently, Et_3N. First, a counterion exchange from Cl^- to NO_3^- was carried out by removing chlorido co-ligands, followed by rearrangement of the structure in a basic environment.[34] The labile NO_3^- anions in the coordination sphere of Pt(II) can be readily replaced under basic conditions, leading to the generation of a two-dimensional lattice with Pt(II) ions bound by four pyridine-N donors, which was demonstrated by strong downfield shifts in the ^{1}H NMR spectrum after this conversion.

Characterization of heterometallic materials

As expected for coordination polymers, their solubility in most solvents was very limited, which effectively hampered their full characterization in solution. Although the ^{1}H NMR spectra for **P1–P3** described above are not readily interpreted, their profiles are consistent with the formation of larger aggregates. High-resolution ESI-MS spectrometry also confirmed the successful generation of the desired heteronuclear complexes. The mass spectra recorded for **P1–P3** demonstrated the presence of the expected fragmentary constituents consisting of chains of successive monomers connected by additional metal ions. All of the identified peaks were in good agreement with their calculated theoretical distribution, allowing the composition and heterometallic nature of the aggregates to be established (Fig. S8, S10 and S12†).

The metal content of the polymeric materials **P1–P3** was determined *via* ICP-MS analysis, which enabled confirmation of the presence of the two different metals expected, *i.e.* Ag and Pd for **P1**; Pd and Pt for **P2**, **P3** (Table S2†). The percentage contribution of individual metal ions corresponds well to the values calculated for each polymer, with minor deviations perhaps attributable to the lack of any means of ensuring sample purity. XPS spectroscopy confirmed the identity of the different metal mixtures in the three heterometallic polymers (Fig. S25–S27†). The XPS spectra of **P1–P3** showed signals indicating the presence of Ag(I), Pd(II), and Pt(II) ions, as well as elements from the organic unit: C, O, N.

To further investigate the complex formation, ATR-FTIR analysis was performed in order to confirm the involvement of specific chemical groups in coordination (Fig. S28–S34†). The absorption bands in the structure of the ligand H**L** have been assigned by the comparison of its spectrum with the spectra of the reference compounds containing the indicative fragments, *i.e.* pinacolone, acetylacetone, pyridine and methyl isonicotinate (Fig. S35†). It resulted in the identification of characteristic band at 1611 cm^{-1} related to the stretching vibration of the C=O bond of β-diketonate unit ($\nu_{C=O}$) and four bands in the region 1585–1427 cm^{-1} from C=N and C=C bond vibrations of the heterocyclic ring (ν_{py}). With regard to the coordination assemblies, their recorded IR spectra were consistent with the assumed bonding modes.[37] For the mononuclear compounds, the shifts of the absorption bands to lower wavenumbers corresponding to β-diketonate (**C6**) or pyridine ring (**C2**, **C4**) demonstrate the existence of the metal coordination bonding and confirm the complexation reaction of the ligand H**L** with the appropriate metal ions, whereas the other bands are observed almost in the same position (Fig. S36†). FTIR spectra show that the generation of the heterometallic polymers **P1–P3** results in the clear red shifts of the bands characteristic of both $\nu_{C=O}$ and ν_{py} vibrations of the ligand functional groups (Fig. 3). Furthermore, in the spectra of **C2**, **C4** and **P1**, we observed the appearance of an additional

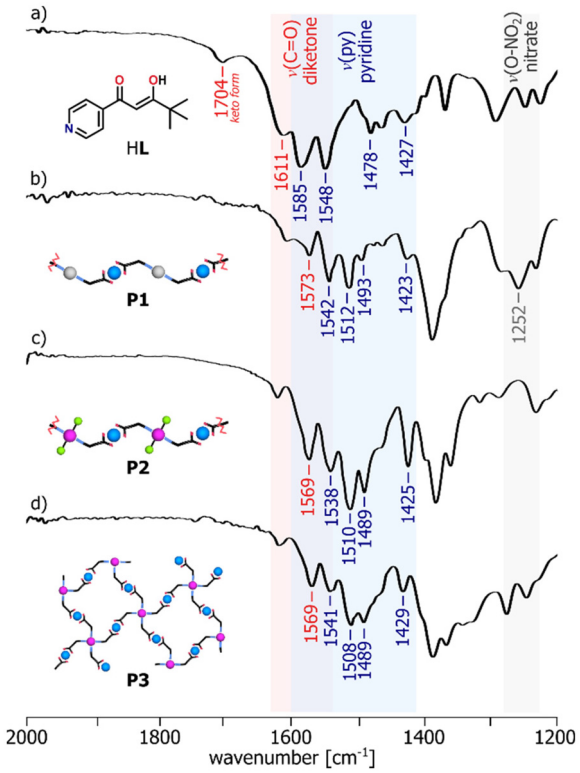

Fig. 3 ATR-FTIR spectra in the 2000–1200 cm^{-1} region of: the ligand **HL** (a) and the polymers **P1–P3** (b–d), showing the involvement of the functional groups in metal binding.

band in the region of 1250–1300 cm^{-1}, originating from the stretching vibrations of the O–NO_2 bond due to the presence of NO_3^- counterions in the complex structures.

The bimetallic materials were also characterized *via* scanning electron microscopy (SEM) to establish their morphology (Fig. S43, S45 and S47†). The images were recorded with an accelerating voltage of 10 kV and magnification up to ×30 000 using an LFD in solid state. The morphologies of the coordination aggregates **P1–P3** indicate the existence of irregular polymer networks depending on their one- or two-dimensional structure. The SEM images of **P1–P3** illustrate the formation of quasi-spherical particles of various sizes in the nanometer range. As shown in Fig. 4, all the species show a tendency to agglomerate into larger clusters and the one-dimensional polymers **P1–P2** intertwine with each other, creating rounded, disordered shapes. For comparison, SEM images were also recorded for the metalloligands **C1**, **C4** and **C6** (Fig. S49–S51†). In contrast to **P1–P3**, the mononuclear complexes appear as single microcrystals with regular shapes. The SEM results are consistent with the data obtained *via* powder X-ray diffraction (pXRD) studies. The pXRD patterns with a set of sharp and intense reflections indicate the crystallinity of the samples **C1**, **C4** and **C6** (Fig. S37–S39†). In contrast, the diffractograms recorded for **P1–P3** established their amorphous character (Fig. S40–S42†), which, however, can be advantageous with regard to their use as (pre) catalysts, facilitating dispersion in the reaction medium.

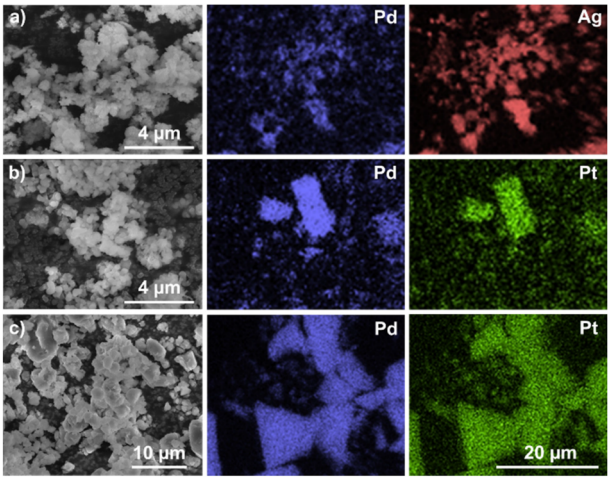

Fig. 4 SEM images and EDS elemental mapping of the sample composition for (a) **P1**; (b) **P2** and (c) **P3**. The same magnification indicated in the graphic was used for all EDS images.

EDS mapping provided the topographic distribution of individual elements in the samples (Fig. 4 and S44, S46, S48†). Comparison of the false-color EDS mapping images demonstrated the uniform and common location of the metal pairs in each solid, consistent with their identity as heterometallic coordination polymers.

Thermogravimetric analysis (TGA) was conducted to study the thermal stability of the compounds **P1–P3** and compare their properties with the metalloligands **C4** and **C6** used as building blocks in their synthesis. The experiments were performed in the temperature range 30–600 °C under N_2 with a heating rate of 10 °C min^{-1}. The TGA curves of the polymeric materials **P1–P3** have similar profiles and show higher stability than the mononuclear analogues **C4** and **C6** (Fig. S52–S57†). In the DTG curves (Fig. S58†), the main peaks which indicate the rate of decomposition are always shifted towards higher temperatures when **P1–P3** are compared to the corresponding mononuclear units, attributed to the retardation of volatilization within the polymers. The heterometallic aggregates show no weight loss of up to ~250 °C, whereas **C4** and **C6** begin to decompose at 160 and 210 °C, respectively. The stepwise decomposition *via* gradual removal of organic components from the structure of compounds **P2–P3** leads to the formation of the mixture of appropriate metal oxides – PdO and PtO_2 as the residue (calcd. 44.76% and found 47.01% for **P2**; calcd 38.53% and found 35.21% for **P3**). The polymer **P1** turned out to be the most stable, as illustrated by the very gentle course of the TGA curve. In the tested temperature range, it underwent thermal degradation only partially, because the weight loss was equal to 24.44% whereas the mixture of thermal decomposition products, *i.e.* PdO and metallic silver in the final residue should constitute 29.84% of the sample mass.

Catalytic studies

The ability to combine in close and ordered proximity different catalytically active metal ions in the polymers pre-

sently described renders them of particular interest for evaluation of the influence of one metal on the activity of another. The remarkable utility of Pd complexes as catalysts for cross-coupling reactions led us to choose familiar reactions of this kind for an initial assessment of the catalytic properties of the polymers and their precursors. The reaction screening revealed a high potential of the polymeric species **P1–P3** to be applied as precatalysts in various Pd-catalyzed C–C coupling reactions, such as the Heck, Suzuki–Miyaura and Sonogashira reactions. Considering the most promising results in the former process, we decided to assess the influence of the compositional differences between homometallic complexes and heterometallic materials on their catalytic activity in this reaction. Thus, the Heck cross-coupling between iodobenzene and styrene catalyzed by **P2** was chosen as a model reaction for the development of reaction conditions. All the optimization procedures are summarized in the ESI, Table S3.† The percentage of Pd in all the structures was determined *via* ICP-MS analysis and the results were used to calculate the catalyst loading. Different variations in terms of solvents and bases were tested using a 0.1 mol% Pd. Of all the combinations, the pair of Et_3N and DMSO gave the expected (*E*)-stilbene in the highest GC yield after 18 h. Further experiments revealed that the catalyst loading could be reduced to relatively low concentration – 0.05 mol%. This concentration was sufficient to guarantee an almost quantitative conversion along with excellent selectivity achievable after 6 h, whereas the use of 0.01 mol% significantly extended the reaction time to 18 h. Taking economic and environmental considerations into account, subsequent catalytic reactions were carried out in DMSO at 100 °C for 6 h using Et_3N (2 equiv.) as a base and 0.05 mol% Pd. Importantly, the reactions were performed without the need to exclude air or water. Furthermore, the metalloaggregates **P1–P3** showed high stability under ambient conditions exceeding several months of storage without any decomposition or loss of catalytic activity, which is beneficial in terms of their utility as catalyst precursors.

A series of catalytic tests was performed to evaluate and compare the performance of other coordination assemblies containing Pd(II) ions in the Heck cross-coupling reaction. For the selected set of aryl iodides and olefins (Fig. 5a), the complex **C6**, a building block of all the coordination polymers, had a lower efficiency under the same total Pd loading (GC yields in the range of 60–68%). Roughly the same results (55–70%) were obtained using a mixture of [Pd(bpm)$_2$] and $PtCl_2$, *i.e.* the constituents of the polymer **P2**, lacking the pyridine units and thus unable to unite under the catalytic reaction conditions. In both cases, the lower GC yields are possibly due to the absence of neighboring metal ions compared to the heterometallic aggregates. A number of catalytic centers in a

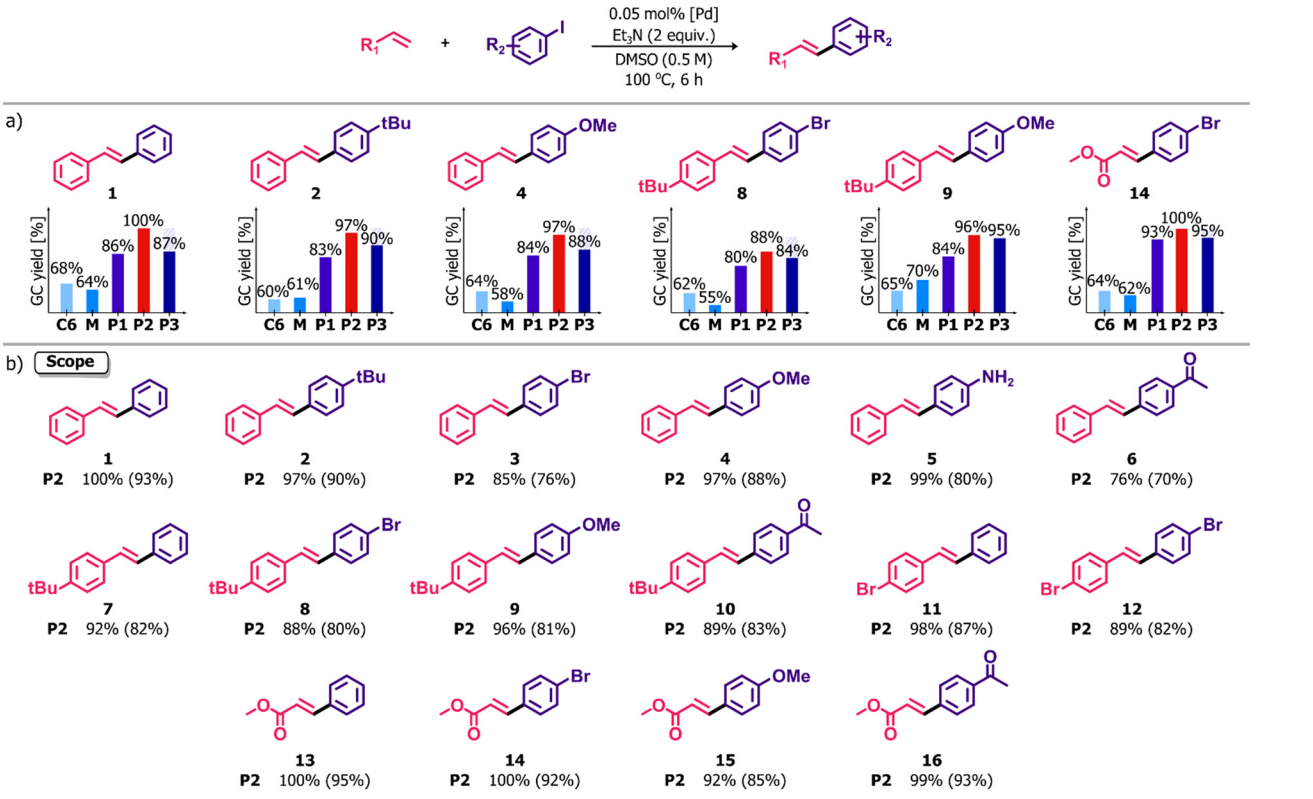

Fig. 5 (a) Comparative tests showing different catalytic activity of the complex **C6**, a mixture of [Pd(bpm)$_2$] and $PtCl_2$ (**M**), and the coordination polymers **P1–P3** in the Heck cross-coupling reaction. (b) Scope of the Heck cross-coupling catalyzed by **P2**. Reaction conditions: aryl iodide (0.5 mmol, 1 equiv.), olefin (0.5 mmol, 1 equiv.), Et_3N (1.0 mmol, 2 equiv.) and the Pd(II) complex (0.05 mol% Pd) were stirred in DMSO (1 mL) at 100 °C for 6 h. Yields determined by GC-MS measurements of aryl iodide decay. The yields in parentheses are those of the isolated compounds.

single molecule significantly increases catalytic activity through a higher local concentration of Pd which is demonstrated in considerably enhanced effectiveness in the reactions catalyzed by **P1–P3**. This positive effect, defined in the literature for dendrimers,[38–41] coordination polymers,[42,43] and recently for polynuclear complexes,[44] was also observed in this case and provides an explanation of the apparent differences between mononuclear units and **P1–P3**. The results of the comparative tests for **P1–P3** demonstrated high efficiency of all the species, slightly variable as indicated by the different reaction yields. The lower catalytic activity of **P3** might be explained due to its morphology since the catalytic sites in the structure of the two-dimensional polymer **P3** might be less accessible compared to its linear counterparts **P1–P2**. Nevertheless, the extension of the reaction time to 12 h allowed attainment of yields comparable to those with the precatalyst **P2**. The local concentration enhancement could possibly be weaker in the case of reactions catalyzed by **P1**. The presence of labile Ag(I) ions as linkers between Pd(II) units might promote polymer fragmentation under reaction conditions that limits the influence of the nuclearity effect. On the other hand, very inert Pt(II) ions are able to retain the polymer structure of **P2** more effectively. Thus, a number of differences between the mononuclear complexes and coordination polymers **P1–P3**, *i.e.* varied nuclearity, composition, dimensionality and morphology, had a significant impact on the course of catalytic reactions and, consequently, on the obtained reaction yields.

With these optimized conditions in hand, we undertook studies of the scope and limitations of this system in the Heck cross-coupling reaction between a series of structurally diversified substrates. The investigations were carried out with the use of **P2** as a catalyst precursor, identified to be the most effective among the investigated. As shown in Fig. 5b, the high efficiency of **P2** was revealed regardless of the presence of electron donating (–OMe, $–NH_2$, –*t*Bu) or electron withdrawing (–COMe, –Br) functional groups in the reactant molecules. In all cases, the stilbene derivatives were formed in high-to-excellent isolated yields, ranging from 70% to 93%. Moreover, the reaction of methyl acrylate with a set of aryl iodides enabled the synthesis of coupling products in excellent yields (85–95%). It is noteworthy that the reaction system exhibited great chemoselectivity towards aryl iodides because no cross-coupling involving bromoarene moieties, as either olefin or haloarene coupling partners, was observed. In all cases, the selectivity in the generation of reaction products with the (*E*)-configuration of double bond was very high and completely independent of the nature of substrates since (*Z*)-isomers never exceeded 10% as determined *via* GC-MS distribution of both isomers.

Conclusions

In summary, the ambidentate nature of the ligand **HL** and its conjugate base $\mathbf{L}^-$ allows the generation of distinct complex compounds with modifiable structure and tunable properties. The availability of free coordination sites enables their utilization as metalloligands in further complexation reactions. The work also defines an effective strategy of coordination-driven structural switching processes for a specific group of coordination systems based on pyridyl-β-diketone ligands. As a consequence, we have successfully synthesized and analyzed new polymeric materials based on precious metals. The structural features, morphology and stability of these coordination assemblies were determined *via* NMR, ESI-MS ICP-MS, XPS, FTIR, SEM-EDS and TG analyses, which unambiguously confirmed their heterometallic character. Furthermore, the coordination polymers reported in this paper exhibit not only structural variety but, more importantly, diverse functionality, as reflected in their catalytic activity. The polymers have been found to be efficient and versatile precatalysts in the Heck cross-coupling reaction within a scope of structurally distinct substrates.

Author contributions

The manuscript was written through contributions of all authors. All authors have given approval to the final version of the manuscript.

Conflicts of interest

There are no conflicts to declare.

Acknowledgements

This research was funded by the National Science Centre in Poland (grant SONATA BIS 2018/30/E/ST5/00032 – ARS).

References

1 E. C. Constable and C. E. Housecroft, *Chem. Soc. Rev.*, 2013, **42**, 1429–1439.
2 W. Wang, Y.-X. Wang and H.-B. Yang, *Chem. Soc. Rev.*, 2016, **45**, 2656–2693.
3 K. Uehara, K. Kasai and N. Mizuno, *Inorg. Chem.*, 2010, **49**, 2008–2015.
4 S. Tashiro, M. Tominaga, T. Kusukawa, M. Kawano, S. Sakamoto, K. Yamaguchi and M. Fujita, *Angew. Chem., Int. Ed.*, 2003, **42**, 3267–3270.
5 J. Beswick, V. Blanco, G. De Bo, D. A. Leigh, U. Lewandowska, B. Lewandowski and K. Mishiro, *Chem. Sci.*, 2015, **6**, 140–143.
6 V. Blanco, A. Carlone, K. D. Hänni, D. A. Leigh and B. Lewandowski, *Angew. Chem., Int. Ed.*, 2012, **51**, 5166–5169.
7 Q.-F. Sun, S. Sato and M. Fujita, *Nat. Chem.*, 2012, **4**, 330–333.

8 S. Hiraoka, T. Yi, M. Shiro and M. Shionoya, *J. Am. Chem. Soc.*, 2002, **124**, 14510–14511.
9 O. Jurček, P. Bonakdarzadeh, E. Kalenius, J. M. Linnanto, M. Groessl, R. Knochenmuss, J. A. Ihalainen and K. Rissanen, *Angew. Chem., Int. Ed.*, 2015, **54**, 15462–15467.
10 H. T. Chifotides and K. R. Dunbar, *Acc. Chem. Res.*, 2013, **46**, 894–906.
11 S. Chen, L.-J. Chen, H.-B. Yang, H. Tian and W. Zhu, *J. Am. Chem. Soc.*, 2012, **134**, 13596–13599.
12 M. Han, R. Michel, B. He, Y.-S. Chen, D. Stalke, M. John and G. H. Clever, *Angew. Chem., Int. Ed.*, 2013, **52**, 1319–1323.
13 V. Blanco, D. A. Leigh and V. Marcos, *Chem. Soc. Rev.*, 2015, **44**, 5341–5370.
14 A. D. Burrows, M. F. Mahon, C. L. Renouf, C. Richardson, A. J. Warren and J. E. Warren, *Dalton Trans.*, 2012, **41**, 4153–4163.
15 C. J. McMonagle, P. Comar, G. S. Nichol, D. R. Allan, J. González, J. A. Barreda-Argüeso, F. Rodríguez, R. Valiente, G. F. Turner, E. K. Brechin and S. A. Moggach, *Chem. Sci.*, 2020, **11**, 8793–8799.
16 G.-L. Wang, Y.-J. Lin, H. Berke and G.-X. Jin, *Inorg. Chem.*, 2010, **49**, 2193–2201.
17 R. G. Pearson, *J. Chem. Educ.*, 1968, **45**, 581–587.
18 T.-L. Ho, *Chem. Rev.*, 1975, **75**(1), 1–20.
19 M. J. Mayoral, P. Cornago, R. M. Claramunt and M. Cano, *New J. Chem.*, 2011, **35**, 1020–1030.
20 A. Walczak, G. Kurpik and A. R. Stefankiewicz, *Int. J. Mol. Sci.*, 2020, **21**(17), 6171.
21 S.-L. Lee, F.-L. Hu, X.-J. Shang, Y.-X. Shi, A. L. Tan, J. Mizera, J. K. Clegg, W.-H. Zhang, D. J. Young and J.-P. Lang, *New J. Chem.*, 2017, **41**, 14457–14465.
22 A. Walczak and A. R. Stefankiewicz, *Inorg. Chem.*, 2018, **57**, 471–477.
23 A. Walczak, H. Stachowiak, G. Kurpik, J. Kaźmierczak, G. Hreczycho and A. R. Stefankiewicz, *J. Catal.*, 2019, **373**, 139–146.
24 R. A. A. Abdine, G. Kurpik, A. Walczak, S. A. A. Aeash, A. R. Stefankiewicz, F. Monnier and M. Taillefer, *J. Catal.*, 2019, **376**, 119–122.
25 M. Dudek, J. K. Clegg, C. R. K. Glasson, N. Kelly, K. Gloe, K. Gloe, A. Kelling, H.-J. Buschmann, K. A. Jolliffe, L. F. Lindoy and G. V. Meehan, *Cryst. Growth Des.*, 2011, **11**, 1697–1704.
26 P. C. Andrews, G. B. Deacon, R. Frank, B. H. Fraser, P. C. Junk, J. G. MacLellan, M. Massi, B. Moubaraki, K. S. Murray and M. Silberstein, *Eur. J. Inorg. Chem.*, 2009, **2009**, 744–751.
27 G.-G. Hou, Y. Liu, Q.-K. Liu, J.-P. Ma and Y.-B. Dong, *Chem. Commun.*, 2011, **47**, 10731–10733.
28 B. Chen, F. R. Fronczek and A. W. Maverick, *Inorg. Chem.*, 2004, **43**, 8209–8211.
29 S. Sanz, H. M. O'Connor, V. Martí-Centelles, P. Comar, M. B. Pitak, S. J. Coles, G. Lorusso, E. Palacios, M. Evangelisti, A. Baldansuren, N. F. Chilton, H. Weihe, E. J. L. McInnes, P. J. Lusby, S. Piligkos and E. K. Brechin, *Chem. Sci.*, 2017, **8**, 5526–5535.
30 H.-B. Wu and Q.-M. Wang, *Angew. Chem., Int. Ed.*, 2009, **48**, 7343–7345.
31 S. Sanz, H. M. O'Connor, P. Comar, A. Baldansuren, M. B. Pitak, S. J. Coles, H. Weihe, N. F. Chilton, E. J. L. McInnes, P. J. Lusby, S. Piligkos and E. K. Brechin, *Inorg. Chem.*, 2018, **57**, 3500–3506.
32 H.-L. Zhu, X.-M. Zhang, X.-Y. Liu, X.-J. Wang, G.-F. Liu, A. Usman and H.-K. Fun, *Inorg. Chem. Commun.*, 2003, **6**, 1113–1116.
33 E. M. Njogu, B. Omondi and V. O. Nyamori, *J. Coord. Chem.*, 2015, **68**, 3389–3431.
34 G. Kurpik, A. Walczak, M. Gołdyn, J. Harrowfield and A. R. Stefankiewicz, *Inorg. Chem.*, 2022, **61**, 14019–14029.
35 N. A. Lewis, S. Pakhomova, P. A. Marzilli and L. G. Marzilli, *Inorg. Chem.*, 2017, **56**, 9781–9793.
36 M. Kołodziejski, A. Walczak, Z. Hnatejko, J. Harrowfield and A. R. Stefankiewicz, *Polyhedron*, 2017, **137**, 270–277.
37 K. Nakamoto, *Infrared Spectra of Inorganic and Coordination Compounds*, Wiley-Interscience, 1970.
38 B. Helms and J. M. J. Fréchet, *Adv. Synth. Catal.*, 2006, **348**, 1125–1148.
39 R. S. Bagul and N. Jayaraman, *J. Organomet. Chem.*, 2012, **701**, 27–35.
40 E. Delort, T. Darbre and J.-L. Reymond, *J. Am. Chem. Soc.*, 2004, **126**, 15642–15643.
41 D. Wang and D. Astruc, *Coord. Chem. Rev.*, 2013, **257**, 2317–2334.
42 M. Kołodziejski, A. J. Brock, G. Kurpik, A. Walczak, F. Li, J. K. Clegg and A. R. Stefankiewicz, *Inorg. Chem.*, 2021, **60**, 9673–9679.
43 S. Kitagawa, R. Kitaura and S.-I. Noro, *Angew. Chem., Int. Ed.*, 2004, **43**, 2334–2375.
44 G. Kurpik, A. Walczak, M. Gilski, J. Harrowfield and A. R. Stefankiewicz, *J. Catal.*, 2022, **411**, 193–199.